Processing of tactile information by the hippocampus

Antonio Pereira*†, Sidarta Ribeiro‡§, Michael Wiest†¶, Leonardo C. Moore†, Janaina Pantoja†, Shih-Chieh Lin†, and Miguel A. L. Nicolelis†‡¶‖††‡‡**

*Departamento de Fisiologia, Universidade Federal do Pará, PA 66075-900, Belém, Brazil; †Department of Neurobiology, ¶Center for Neuroengineering, ‖Department of Biomedical Engineering, and **Department of Cognitive and Brain Sciences, Duke University, Durham, NC 27710; ‡Edmond and Lily Safra International Institute of Neuroscience of Natal, RN 59066-060, Natal, Brazil; §Departamento de Fisiologia, Universidade Federal do Rio Grande do Norte, RN 59072-970, Natal, Brazil; and ††Laboratory of Neural Ensemble Technology, École Polytechnique Fédérale de Lausanne, CH-1015 Lausanne, Switzerland

Communicated by Jon H. Kaas, Vanderbilt University, Nashville, TN, September 11, 2007 (received for review June 29, 2007)

The ability to detect unusual events occurring in the environment is essential for survival. Several studies have pointed to the hippocampus as a key brain structure in novelty detection, a claim substantiated by its wide access to sensory information through the entorhinal cortex and also distinct aspects of its intrinsic circuitry. Novelty detection is implemented by an associative match–mismatch algorithm involving the CA1 and CA3 hippocampal subfields that compares the stream of sensory inputs received by CA1 to the stored representation of spatiotemporal sequences in CA3. In some rodents, including the rat, the highly sensitive facial whiskers are responsible for providing accurate tactile information about nearby objects. Surprisingly, however, not much is known about how inputs from the whiskers reach CA1 and how they are processed therein. Using concurrent multielectrode neuronal recordings and chemical inactivation in behaving rats, we show that trigeminal inputs from the whiskers reach the CA1 region through thalamic and cortical relays associated with discriminative touch. Ensembles of hippocampal neurons also carry precise information about stimulus identity when recorded during performance in an aperture-discrimination task using the whiskers. We also found broad similarities between tactile responses of trigeminal stations and the hippocampus during different vigilance states (wake and sleep). Taken together, our results show that tactile information associated with fine whisker discrimination is readily available to the hippocampus for dynamic updating of spatial maps.

multielectrode recording | rat | somatosensory | width discrimination | sensory pathways

Rats are nocturnal food gatherers that rely on exquisite navigation skills to explore their environment (1). Such navigation is heavily dependent on the use of facial vibrissae, which are extremely sensitive tactile organs used as both high-resolution tactile discriminators (2, 3) and distance detectors (4, 5). During exploration, the vibrissae are bilaterally swept against objects and obstacles to gather accurate information about the animal's close surroundings (2–5). At present, there is abundant evidence that the mammalian hippocampus plays an important role in navigation by creating a map-like representation of the spatial environment (6–8). To be useful, however, this map needs to be constantly updated whenever something changes in the outside world. Several studies have shown that the hippocampus and other structures in the medial temporal lobe are crucially involved with novelty detection (9–12). Novelty detection calls for a system that is able to hold detailed models of the environment and keep track of changes that violate predictions of this model. The hippocampal CA1 field provides just this type of system by comparing sensory inputs from the entorhinal cortex with information stored in the CA3 field (13). Surprisingly, however, despite the wealth of anatomical connections indirectly linking the hippocampus to sensory areas in the cerebral cortex (14), little is known about the processing of sensory signals in this part of the brain. In the particular case of the rat, an important model for sensory neuroscience, tactile responses of neuronal ensembles have never been studied in detail in the hippocampus. Here we set out to quantitatively investigate these responses in the CA1 region of behaving rats. As a comparison, we simultaneously recorded tactile responses in both thalamic and primary cortical relays of the trigeminal lemniscal pathway. Our results show that the response profile of CA1 neuronal ensembles is consistent with the role of the hippocampus as a novelty detector.

Results

Rats ($n = 13$) were implanted with microwire multielectrode arrays in the CA1 region of the hippocampus, the thalamic ventral posteromedial nucleus (VPM), and the primary somatosensory cortex (S1) (Fig. 1*A*). Both extracellular single-unit and local field potential (LFP) recordings were obtained from the same electrodes. To evoke tactile responses with millisecond precision, stimulation was produced by electric current pulses delivered by cuff electrodes (every 10 s, on average, with a random distribution; see *Materials and Methods*; also see Fig. 1*B*) to the right infraorbital (IO) nerve (15), which carries information from the whiskers' mechanoreceptors to the brain (16).

While the IO nerve was being stimulated in the awake, behaving animals, 52% (34 of 65) of CA1 cells, 49% (82 of 167) of S1 cells, and 32% (18 of 56) of VPM cells were responsive to the electrical stimulation. Based on the level of ongoing neuronal activity, 60.0% (39 units) of CA1 responses were excitatory, whereas 40.0% (26 units) were defined as multimodal responses having an inhibitory phase followed by an excitatory one. These proportions were not different in VPM [excitatory, 67.86% (38 units); multimodal, 32.14%] (18) and S1 [excitatory, 72.45% (121 units); multimodal, 27.55% (46 units)] ($P > 0.6$) (see Fig. 1*C*). Evoked responses in CA1 had average latencies that were more than twice as long as the ones in S1 and VPM (18.09 ± 0.97 ms vs. 8.56 ± 0.51 and 7.25 ± 0.21 ms, respectively) ($P = 0.00002$) (Fig. 1*D*). Also, the average amplitude of electrically evoked responses was not significantly different when comparing unit recordings in the three relays (Fig. 1*E*).

Altogether, these results are consistent with the notion that tactile inputs reach CA1 by way of the somatosensory trigeminal pathway. To further test this hypothesis, we recorded electrically evoked responses in CA1 before and after the inactivation of S1 and/or VPM with 0.2 μl of 1% muscimol, a potent GABA agonist that induces local, reversible neural inactivation for ≤12 h (17). On average, S1 inactivation decreased the amplitude of evoked responses in CA1 cells by 54.57 ± 8.05% ($n = 12$ units) (Fig. 2 *A* and *D*). Muscimol injection in both S1 and VPM nearly abolished evoked activity in CA1 (99.6 ± 0.13% reduction; $n =$

Author contributions: A.P. and S.R. designed research; A.P., M.W., L.C.M., and J.P. performed research; A.P., M.W., S.-C.L., and M.A.L.N. contributed new reagents/analytic tools; A.P. and M.W. analyzed data; and A.P., S.R., and M.A.L.N. wrote the paper.

The authors declare no conflict of interest.

Freely available online through the PNAS open access option.

Abbreviations: IO, infraorbital; LFP, local field potential; LVQ, learning vector quantization; QWK, quiet waking; REM, rapid eye movement; S1, primary somatosensory cortex; SWS, slow-wave sleep; VPM, ventral posteromedial nucleus.

‡‡To whom correspondence should be addressed. E-mail: nicoleli@neuro.duke.edu.

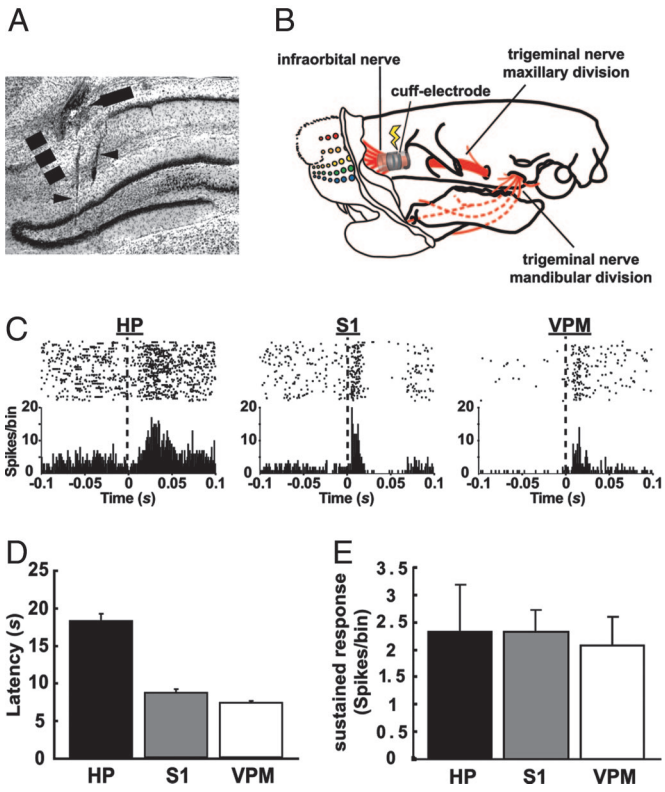

Fig. 1. Electrically evoked tactile responses in the CA1, S1, and VPM. (*A*) Localization of electrode tracks in a frontal section of the hippocampus stained with cresyl violet. We used a staggered electrode array targeting both CA1 (arrow) and the dentate gyrus (DG) of the hippocampus (arrowheads), the latter being one of the sources of LFPs for the determination of vigilance state (see *Materials and Methods*). The dashed line marks the CA1/subiculum border. (*B*) Schematic diagram showing the location of the cuff electrode implant used to stimulate the IO nerve in behaving rats. (*C*) Representative single-unit, electrically evoked responses in CA1, S1, and VPM. (*Upper*) Raster plot of unit spikes, with each line representing a consecutive stimulation trial. (*Lower*) Summed activity for all trials in 1-ms bins. For data analyses, the initial 2 ms were eliminated to discard electrical stimulus artifacts. HP, hippocampus. (*D*) Mean ± SEM latencies of electrically evoked responses in CA1, S1, and VPM ($n = 3$ animals). Response latency to electrical stimulation was estimated as the third peristimulus time histogram consecutive bin, with values falling outside the 95% confidence interval ($P < 0.05$) of a Poisson distribution fitted to the previous 100-ms interval baseline. (*E*) Mean ± SEM amplitude of electrically evoked sustained responses in CA1, S1, and VPM ($n = 3$ animals). This response was calculated by integrating the firing rate over a period of 2–50 ms after the stimulus, subtracted from the average firing rate during the 100-ms preceding the stimulus (15).

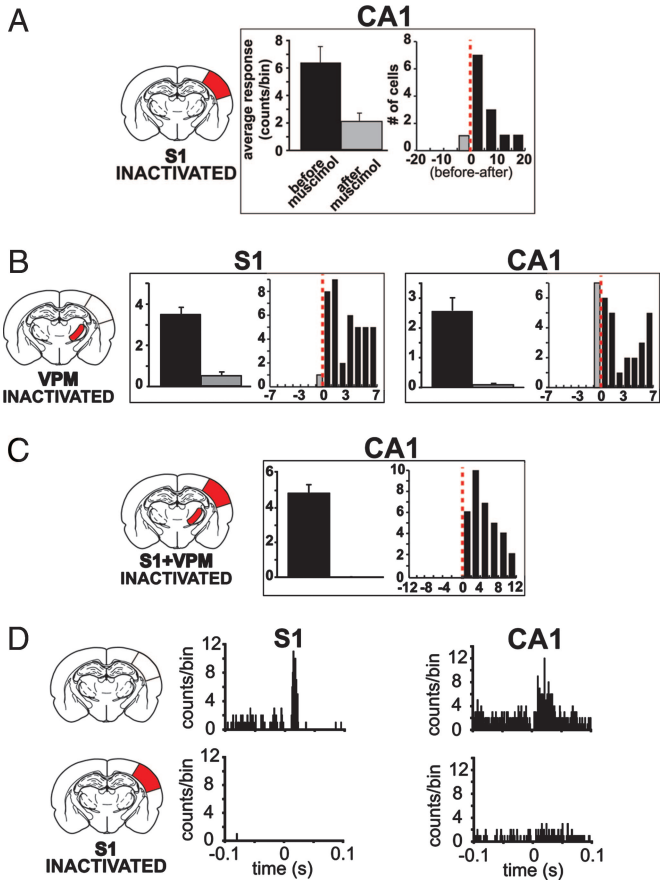

Fig. 2. Tactile responses in CA1 depend on the integrity of the somatosensory lemniscal pathway. Muscimol (0.1%) was injected into S1 (*A* and *D*), VPM (*B*), or both (*C*), and the effects were measured on CA1 units after stimulation of the IO nerve. (*A*) The left histogram shows muscimol injection caused a great reduction on electrically evoked responses (mean ± SEM) of CA1 units (average of two cases). The right histogram shows the effects of muscimol on sampled units through the difference between average cell activity before and after the injection (red dashed line indicates no difference). (*B*) Injection of muscimol into the VPM disrupts tactile processing in S1 as expected but also causes a much stronger reduction in CA1 unit activity than inactivation of S1 only (compare with *A*). (*C*) Muscimol injection into both S1 and VPM brings about a complete reduction in CA1 unit activity. (*D*) Peristimulus time histograms of two representative units showing the effects of S1 inactivation on electrically evoked response in S1 and CA1. See Fig. 1 legend for description of peristimulus time histogram plots.

34 units) (Fig. 2*C*), but so did the inactivation of VPM only (99.36 ± 6.7% reduction; $n = 31$ units), which also caused a great reduction of evoked activity in S1 cells (88.36 ± 3.27% reduction; $n = 41$ units) (Fig. 2*D*).

Direct electrical stimulation of the hippocampus by way of the perforant path has been shown to produce state-dependent responses that vary according to wake and sleep states (18, 19). Because tactile responses in both S1 and VPM are strongly modulated by rats' global behavioral state (15), we tested whether tactile responses in CA1 are similarly modulated. Three animals were continuously recorded for ≤36 h while the right IO nerve was being electrically stimulated by a cuff electrode so as to obtain sufficient samples of single-unit evoked responses during quiet waking (QWK), slow-wave sleep (SWS), and rapid eye movement (REM) sleep. Spectral state maps (20) were used for the quantitative, automated sorting of the three vigilance states (Fig. 3*A*). The evoked responses obtained in all three areas varied substantially according to the animal's vigilance state (Fig. 3*B*). When normalized to the waking state, there was a significant increase in response amplitude during sleep in CA1 ($n = 59$ units): SWS (3.79 ± 0.63, $P < 0.0001$) and REM (2.82 ± 0.43, $P < 0.0001$); S1 ($n = 110$ units): SWS (4.94 ± 0.64, $P < 0.0001$) and REM (3.63 ± 0.38, $P < 0.0001$); and VPM ($n = 33$ units): SWS (11.92 ± 7.17, $P < 0.0001$) and REM (9.25 ± 5.71, $P < 0.0001$). Additional quantitative analysis of these data indicates that electrical stimulation during sleep evoked larger responses during SWS than REM sleep for both CA1 ($P < 0.0001$) and S1 ($P < 0.0001$), but not for VPM ($P > 0.05$). Strength of sleep-dependent responses was similar in S1 and VPM (SWS, $F = 6.11$, $P > 0.05$; REM, $F = 5.03$, $P > 0.05$), but decayed in CA1 (SWS, $F = 6.11$, $P < 0.01$; REM, $F = 5.03$, $P < 0.01$). These results are in line with findings obtained with direct stimulation of the perforant path in awake animals (19) and suggest that the active gating of tactile responses observed in VPM and S1 also takes place in CA1 (15).

NEUROSCIENCE

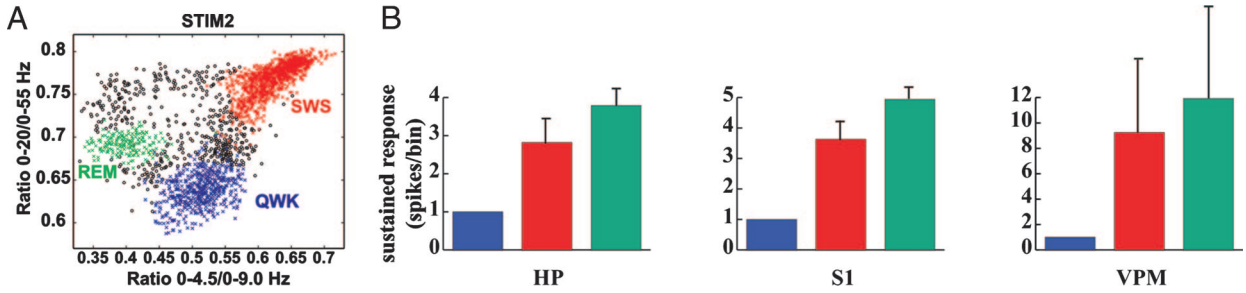

Fig. 3. State dependency of electrically evoked responses in CA1, S1, and VPM. (*A*) State-space map for one subject (STIM 2) recorded over 24 h (20). Each symbol (filled circle or ×) represents a 1-s epoch of recorded LFPs. The scatter plot is built from two LFP spectral ratios (20). Three distinct clusters corresponding to different states on the wake–sleep cycle are visible: QWK, SWS, and REM sleep. The colored symbols (×) correspond to electrical stimuli delivered to the IO nerve during epochs pertaining to each of these states (blue, QWK; red, SWS; green, REM). (*B*) Average amplitude (mean ± SEM) of evoked responses of hippocampal, S1, and VPM cells during the three vigilance states in all subjects analyzed. In every recorded area, the electrical stimuli evoked stronger responses when animals were sleeping than during waking. Quantitative analysis of evoked responses is similar to Fig. 1. HP, hippocampus.

Given the above results showing that evoked responses in HP are qualitatively similar to S1/VPM and tactile responses in S1 differ when whiskers are either actively or passively stimulated (2), we decided to further investigate whether activity of single units in CA1 carry specific information about stimulus identity in behaving animals. Rats were submitted to two separate stimulation protocols. In the first protocol, head-fixed animals ($n = 2$) had their whiskers stimulated passively by a sliding aperture (Fig. 4*A*) (2). The second protocol used an active discrimination task, in which freely moving animals ($n = 5$) were tested on a width discrimination paradigm (Fig. 4*B*) (3).

Robust neuronal responses in CA1 (active, $n = 52$ units; passive, $n = 15$ units) were observed in both protocols (Fig. 4 *C* and *D*), with significantly stronger responses (9.7 ± 3.7 spikes per trial) during active whisking, compared with passive stimulation (3.77 ± 0.16 spikes per trial) ($t_{58} = 14.28, P < 0.00001$) (Fig. 4*D*). The duration of tactile-evoked responses in the hippocampus was longer during active discrimination (338.46 ± 20.09 ms) than with passive stimulation (77.93 ± 8.43 ms) ($t_{63} = 11.96$, $P < 0.00001$) (Fig. 4*C*). The same was true for S1 (active, 240.28 ± 13.34 ms; passive, 41.89 ± 5.86 ms) ($t_{123} = 13.61$, $P < 0.00001$) (Fig. 4*C*). Also, the duration of CA1 responses was significantly longer than S1 responses for both protocols (active, $t_{97} = 4.07$, $P < 0.00001$; passive, $t_{26} = 3.51$, $P < 0.01$) (Fig. 4*C*).

To evaluate the presence of stimulus-related information in the activity of both CA1 and S1 neuronal ensembles during the active discrimination task, we used an artificial neural network for pattern recognition based on the learning vector quantization (LVQ) algorithm (see *Materials and Methods*) (21). We compared the average ($n = 5$ animals) artificial neural network discrimination performance in the last time window before the rat's whiskers contacted the aperture (0.4-s window starting at −0.5 s) (see Fig. 4*E*) to performance during subsequent windows. As expected (2), the average S1 ensemble's performance rose significantly above prestimulus levels in the first poststimulus window, beginning at 0.0 s ($t_4 = 8.8$, $P < 0.0001$). CA1 neuronal ensembles also carry information about stimulus identity because they were able to discriminate between the narrow and wide apertures to an extent similar to S1, but reached statistical significance only on the third poststimulus window, starting at 0.2 s ($t_4 = 5.15$, $P < 0.01$). Inspection of individual subjects' performances indicates that the delay to reach significance in the discrimination performance of the hippocampus ensemble activity (≈0.2 s) is not merely because of higher between-subject variability, but rather reflects an actual delay in hippocampus tactile processing consistent with information being relayed from S1 to the hippocampus. Recently, our group has shown that reversible inactivation of the hippocampus with muscimol during the gap discrimination task brings the rats' performance to chance level (D. J. Krupa, M.W., and M.A.L.N., unpublished data).

Discussion

In the present work, we investigated the nature, origin, and state dependency of tactile responses in the CA1 region of the hippocampus of behaving rats. These experiments show that neurons in the behaving rats' hippocampus react with a high degree of selectivity to whisker stimulation, and that its inputs originate from components of the trigeminal pathway associated with discriminative touch, which includes VPM and S1. We also showed that tactile responses in CA1 are subject to the same systemic state modulation that constrains tactile responses in S1, including sleep, strengthening the notion that tactile processing in the hippocampus is located downstream to the lemniscal pathway, configuring an integrated cortical-hippocampal circuit. In our awake animals experiments, the tactile-evoked responses of CA1 units have a profile that is surprisingly similar to the ones recorded in S1 (2). For instance, responses in CA1 are enhanced when tactile stimuli are salient in the context of a discriminative task (Fig. 4 *A* and *B*) and do not depend on movements of the head or body because they also occur when the head of the animal is fixed (Fig. 4*A*). These findings highlight the importance of applying to the hippocampus the same systemic approach that allowed great progress in understanding the basic rules of information processing in sensory areas, both cortical and subcortical. We have many hypotheses about what the hippocampus might be doing, but comparatively fewer data about how it might be doing it. A good example of this issue is provided by the cognitive map theory.

The existence of place cells in the rodent hippocampus, which are characterized by location-specific firing (22), provided the original premise behind the highly influential cognitive map theory of hippocampal function (7). The spatial code generated by place cells is informed by sensory inputs from several modalities (23), signaling both allothetic (external) and idiothetic (self-motion) cues. Allothetic cues can be located either distal or proximal to the animal and help form the viewpoint-independent, allocentric representation of space in the hippocampus. Surprisingly, however, the role of proximal cues in defining the firing fields of place cells has not been systematically investigated, being overlooked in experimental studies in favor of distal, mostly visual determinants despite the fact that vision does not seem to be necessary for the spatial firing properties of place cells (23). In fact, nonvisual cues, such as haptic information, can compensate for the lack of visual signs in inducing spatially coherent firing in the hippocampus (23, 24). For instance, in a situation where visual information is not available and the rat must rely on its whiskers to navigate, knowledge of

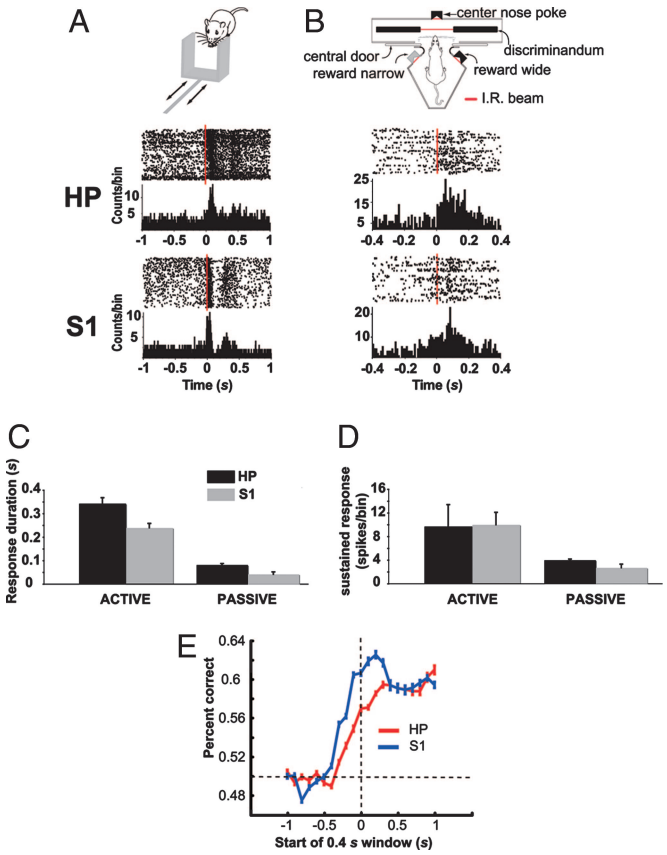

Fig. 4. Responses of hippocampal cells to mechanical stimulation of the whiskers in awake and behaving animals. (*A*) Tactile responses in CA1 and S1 to the passive stimulation of the whiskers. (*Top*) Schematic of a moving aperture stimulus. The aperture is accelerated across the facial whiskers by a pneumatic solenoid (2). (*Middle* and *Bottom*) The response of two representative cells recorded in CA1 and S1, respectively, to the passive stimulation (see Fig. 1 legend for a description of plots). Bin size, 10 ms. The zero time point represents stimulus onset (vertical dashed line). HP, hippocampus. (*B*) (*Top*) Schematic of testing chamber used during the active discrimination protocol (see *Material and Methods*). (*Middle* and *Bottom*) Responses of two representative cells in CA1 and S1. Bin size, 10 ms. (*C* and *D*) Mean ± SEM response duration and magnitude, respectively, of CA1 and S1 cells evoked during active discrimination and passive whisker stimulation. Amplitude of sustained response was calculated by integrating the firing rate over a period of 300 ms subtracted from the average firing rate during the 100 ms preceding the IR beam breaking. (*E*) Average LVQ output (one recording session per animal) ($n = 5$ animals) for CA1 and S1 showing the ability to discriminate between the wide and narrow gap based on the recorded population activity before and after whiskers contacted the aperture. Before the whiskers contacted the aperture, the ability of the LVQ to discriminate between the two apertures was near chance (horizontal dashed line). After the whiskers contacted the aperture, the performance of the LVQ classifier improved above chance for both CA1 and S1 (see *Results*). The classifier performance for S1 peaked before CA1 (see *Results*).

the intrinsic properties of explored objects is essential to allow the reconstruction of the firing field of place cells (23). As our results have shown, the whiskers' inputs reaching the hippocampus have the required response selectivity (25) to help the rat navigate adequately and provide accurate information about nearby objects to place cells.

Despite the overwhelming success of the cognitive map theory, there has been intense dispute about the role played by the human hippocampus and adjacent structures of the medial temporal lobe in memory: Is it really specialized for spatial memories (26) or does it have a more general role in declarative memory as a stimulus association detector (27)? Increasingly, it is becoming evident that the second option is more correct: The hippocampus is a complex sensory hub associated with declarative memory in general, working memory, novelty detection (26), and even perception (10, 28–33). In each of these instances, the hippocampus needs to have access to detailed information about the environment provided by a constellation of sensory stimuli. The putative role of the hippocampus in novelty detection provides such an example. According to this proposal, when an animal navigates through a familiar route, the incoming stream of peripheral sensory information is parsed by CA1 in search of novelty (10, 11). Novelty is detected by CA1 as any significant deviation from the stimulus-associative predictions established by the contextual model stored in the CA3 region (11, 13, 34). The CNS uses the outcome of this computation to select the appropriate behavioral response to deal with the current context (35). The adaptive advantage conferred by novelty detection is obvious and, among other things, could help animals detect camouflaged predators.

Sensory information used for novelty detection arrives in the temporal lobe through both uni- and polymodal cortical sensory areas (14, 36). Information about individual stimuli originates from unimodal sensory areas, such as S1, and is forwarded to the hippocampus through the perirhinal cortex and lateral entorhinal area (14, 36, 37). Contextual information related to the spatial arrangement of distinct objects, in contrast, reaches the hippocampus through the parahippocampal cortex and medial entorhinal area (14, 36, 37). From the entorhinal area, where both pathways converge, sensory stimuli reach the hippocampus through the perforant path, which targets the CA1 and CA3 fields. Through an associative match–mismatch mechanism, sensory information dynamically represented in CA1 is compared with contextual information stored in CA3 (11, 13, 34).

Novelty detection also is useful to illustrate the general role played by the hippocampus in memory processing, especially working memory (38–40). To categorize a stimulus as novel or salient, it is necessary to hold and associate stimulus information over brief temporal intervals. Our findings show that CA1 is capable of discriminating tactile stimuli in a nonspatial task, of which the successful performance depends on a sensory cue to be transiently stored in short-term memory (see Fig. 4*B*). As expected, the hippocampus is extensively interconnected with areas in the prefrontal cortex subserving working memory (41).

Involvement of the hippocampus with sensory processing also is emphasized by its association with schizophrenia (42, 43). Hallucinations which involve abnormal sensory experiences that are unrelated to external events, are one of the hallmarks of schizophrenia. Early anatomical data have already shown that the hippocampus is reduced in volume in schizophrenic patients (43). Also, functional MRIs have shown strong activation in medial temporal lobe structures, especially the hippocampus, of schizophrenic patients during hallucinatory episodes (44).

Materials and Methods

Multielectrode Implants. The surgical procedures for electrode implantation (including the cuff electrode) were done while the rats were anesthetized with 100 mg/kg ketamine and 8 mg/kg xylazine and are described in detail elsewhere (2, 15, 45). The rats were placed in a stereotaxic head holder, and two small craniotomy windows were made over the localization of the barrel cortex and the VPM (one of the arrays consisted of staggered microwires designed to reach CA1 and the VPM). Two arrays of 32 microelectrodes built from 35-μm-diameter Teflon-coated tungsten microwires (1.5 MOhm at 1.0 KHz) were stereotaxically implanted in the brain aiming for the S1 posteromedial barrel subfield, the VPM, and the dorsal part of the hippocampal CA1 region according to the following coordinates (in millimeters): CA1 [anterior/posterior (AP), +2.8; medial/

lateral (ML), +1.5; dorsal/ventral (DV), −3.3], S1 (AP, +3.0; ML, +5.5; DV, −1.5), and VPM (AP, +3.0; ML, +3.0; DV, −5.0) (46). One of the arrays was built to reach both CA1 and the VPM, with each being contacted by 16 microwires.

Electrical Stimulation, Electrophysiological Recordings, and State Identification. Details of experimental procedures and analysis can be found in earlier reports (2, 15, 20, 47). Subjects were three 300- to 350-g adult female Long–Evans rats. Briefly, 1–4 mA, 100-μs, single-current electrical stimuli were delivered on average every 10 s, according to a Poisson distribution, to cuff electrodes surgically implanted around the IO nerve (15). The animals did not seem to be particularly distressed with electrical stimuli during any of the vigilance states. Single-unit activity was recorded from microelectrode arrays while animals were kept in a soundproof chamber for ≤36 h, and behavior was recorded with infrared CCD cameras (WV-BP332; Panasonic, Suwanee, GA). Neural signals were preamplified 2,000–32,000×, digitized at 40 kHz, and sorted according to the following cumulative criteria: (*i*) voltage thresholds >2 SDs of amplitude distributions, (*ii*) signal-to-noise ratio >2.5 (verified on the oscilloscope screen), (*iii*) <1% of interspike intervals <1.2 ms, and (*iv*) stereotypy of waveform shapes as determined by a waveform template algorithm and principal component analysis. For long recordings (≤36 h), we used an adaptive algorithm (SortClient; Advanced Intellect LLC, Custer, WI) that adjusts units' waveform templates over time based on the recently accumulated mean shapes. LFPs were recorded from the same electrodes, preamplified 1,000×, filtered at 0.5–400 Hz, and digitized at 500 Hz. Three global brain states, QWK, SWS, and REM (20), were identified and quantified by an automated spectral analysis of LFP signals that used 0.5–2- to 0.5–55-Hz and 0.5–4.5- to 0.5–9-Hz frequency ratios as orthogonal axes of a state map that reliably separated them according to their characteristic spectral dynamics (20).

Muscimol Inactivation. Subjects were three 300- to 350-g adult female Long–Evans rats. Briefly, 0.1% muscimol in 0.9% saline was infused into the VPM and/or the S1 posteromedial barrel subfield through a 33-gauge infusion cannula lowered through a guide tube glued to the multielectrode arrays. The cannula stood 0.2 mm above the electrode tips. Muscimol infusion lasted for 5 min up to a volume of 0.5 μl while animals were under light halothane anesthesia. Recordings began 1 h after anesthesia's offset. First, electrically evoked neuronal activity was recorded for ≈3 h to serve as a baseline. Then muscimol was injected. After recovering from anesthesia, the animal returned to the recording chamber for 3 h of additional recording. Previous reports showed that muscimol inactivation of S1 cortex, by using similar drug volumes, lasted for at least 6 h (45). Muscimol inactivation spread over a diameter of ≈1.4 mm (48). Although this finding assured that most of the posteromedial barrel subfield and VPM were inactivated, it is possible that the posteromedial nucleus, which receives input from the whiskers and is part of the paralemniscal pathway (25), also is affected during injections centered in the VPM.

Active Whisker Stimulation. Subjects were five 300- to 400-g adult Long–Evans female rats. Water-deprived rats were trained to use their long facial whiskers to discriminate between a wide (72-mm) and narrow (60-mm) aperture to receive a 50-μl water reward (2, 3). The intertrial interval was set at 10 s. When the rats reached performance criterion (at least 75% accuracy for three consecutive sessions), water restriction was interrupted, and microelectrode arrays were surgically implanted in the VPM, S1, and hippocampus. Seven days later, the animals were recorded electrophysiologically while performing the discrimination task. We recorded from 52 units in the hippocampus, 87 units in S1, and 29 units in the VPM.

The relationship between the neuronal ensemble's behavior and task performance was quantified by using a nonparametric statistical pattern-recognition method, the optimized LVQ (2, 21, 47, 49), with learning rule implemented by code available in Matlab (Mathworks, Natick, MA), and the Matlab Neural Network Toolbox (Mathworks) (50). Single-trial 100-ms bin peristimulus time histograms were constructed for 400-ms epochs defined relative to the time when the rats sampled the tactile stimuli. Data sets were divided into training and testing subsets. Results were quantified in terms of percentage of single trials classified correctly. A moving window analysis was used to assess the time course of information about the wide and narrow apertures. LVQ was applied sequentially to a 400-ms epoch of neuronal ensemble activity that moved in 100-ms steps through the 1-s epochs before and after the time of whisker contact. This analysis demonstrated a continuous quantitative readout of the recorded population's ability to distinguish between the wide and narrow apertures.

Passive Whisker Stimulation in Awake Rats. Subjects were two 300- to 350-g female Long–Evans adult rats. Rats were head restrained and had a movable aperture sweep across their whiskers in a manner that simulated a single sweep of the whiskers' deflections occurring during active discrimination (2). Rats were habituated to physical restraint, and each rat received at least 200 stimuli delivered with a random interstimulus interval. Single unit activity and LFPs were recorded simultaneously from the VPM, S1, and hippocampus, as described above.

Data Analyses. Differences on the latency of evoked responses and differences on both the amplitude and duration of neuronal responses were compared among groups (according to vigilance state, recorded area, and whisker stimulation protocol) by using ANOVA and Student's two-tailed *t* test. When appropriate, post hoc analysis was carried out with a Newman–Keuls test. The criterion for statistical significance was preset at an α level of 0.05 (15). Average values are expressed as mean ± SEM.

Histology. The 30-μm frontal brain sections stained with cresyl violet were used to confirm the anatomical placement of multielectrode arrays in CA1, VPM, and S1.

We thank Gary Lehew and Jim Meloy for outstanding technical support; Erika Fanselow for help making the cuff electrodes; Jennifer Stapleton and Marco Aurelio Freire for help with statistics; Eric E. Thomson for suggestions in the manuscript; Ivan Araújo and Jonathan Ross for help with programming; and Susan Halkiotis for proofreading the manuscript. This work was supported by a Pew Latin America Fellowship (to S.R.) and National Institutes of Health Grants 5 R01 DE11451 and 5 R01 DE 13810 (to M.A.L.N.).

1. Nowak RM (1999) *Walker's Mammals of the World* (Johns Hopkins Univ Press, Baltimore).
2. Krupa DJ, Wiest MC, Shuler MG, Laubach M, Nicolelis MA (2004) *Science* 304:1989–1992.
3. Krupa DJ, Matell MS, Brisben AJ, Oliveira LM, Nicolelis MA (2001) *J Neurosci* 21:5752–5763.
4. Brecht M, Preilowski B, Merzenich MM (1997) *Behav Brain Res* 84:81–97.
5. Carvell GE, Simons DJ (1990) *J Neurosci* 10:2638–2648.
6. Ekstrom AD, Kahana MJ, Caplan JB, Fields TA, Isham EA, Newman EL, Fried I (2003) *Nature* 425:184–188.
7. O'Keefe J, Nadel L (1978) *The Hippocampus as a Cognitive Map* (Oxford Univ Press, Oxford).
8. Wilson MA, McNaughton BL (1993) *Science* 261:1055–1058.
9. Dolan RJ, Fletcher PC (1997) *Nature* 388:582–585.
10. Knight R (1996) *Nature* 383:256–259.
11. Kumaran D, Maguire EA (2006) *PLoS Biol* 4:e424.

12. Ranganath C, D'Esposito M (2001) *Neuron* 31:865–873.
13. Lee I, Yoganarasimha D, Rao G, Knierim JJ (2004) *Nature* 430:456–459.
14. Burwell RD, Amaral DG (1998) *J Comp Neurol* 398:179–205.
15. Fanselow EE, Nicolelis MA (1999) *J Neurosci* 19:7603–7616.
16. Dorfl J (1985) *Journal of Anatomy* 142:173–184.
17. Krupa DJ, Ghazanfar AA, Nicolelis MA (1999) *Proc Natl Acad Sci USA* 96:8200–8205.
18. Winson J, Abzug C (1978) *J Neurophysiol* 41:716–732.
19. Winson J, Abzug C (1977) *Science* 196:1223–1225.
20. Gervasoni D, Lin SC, Ribeiro S, Soares ES, Pantoja J, Nicolelis MA (2004) *J Neurosci* 24:11137–11147.
21. Laubach M, Wessberg J, Nicolelis MA (2000) *Nature* 405:567–571.
22. O'Keefe J, Dostrovsky J (1971) *Brain Res* 34:171–175.
23. Save E, Cressant A, Thinus-Blanc C, Poucet B (1998) *J Neurosci* 18:1818–1826.
24. Quirk GJ, Muller RU, Kubie JL (1990) *J Neurosci* 10:2008–2017.
25. Ahissar E, Sosnik R, Haidarliu S (2000) *Nature* 406:302–306.
26. Shrager Y, Bayley PJ, Bontempi B, Hopkins RO, Squire LR (2007) *Proc Natl Acad Sci USA* 104:2961–2966.
27. Fortin NJ, Agster KL, Eichenbaum HB (2002) *Nat Neurosci* 5:458–462.
28. Eichenbaum H (2004) *Neuron* 44:109–120.
29. Vinogradova OS (2001) *Hippocampus* 11:578–598.
30. Vannucci M, Grunwald T, Pezer N, Dietl T, Helmstaedter C, Schaller C, Viggiano MP, Elger CE (2006) *Neurosci Lett* 401:165–170.
31. Fortin NJ, Wright SP, Eichenbaum H (2004) *Nature* 431:188–191.
32. Eichenbaum H (2003) *Trends Cogn Sci* 7:427–429.
33. Lee AC, Buckley MJ, Gaffan D, Emery T, Hodges JR, Graham KS (2006) *J Neurosci* 26:5198–5203.
34. Lisman JE (1999) *Neuron* 22:233–242.
35. Guzowski JF, Knierim JJ, Moser EI (2004) *Neuron* 44:581–584.
36. Witter MP, Groenewegen HJ, Lopes da Silva FH, Lohman AH (1989) *Prog Neurobiol* 33:161–253.
37. Daselaar SM, Fleck MS, Cabeza R (2006) *J Neurophysiol* 96:1902–1911.
38. Knowlton BJ, Fanselow MS (1998) *Curr Opin Neurobiol* 8:293–296.
39. Sarnthein J, Petsche H, Rappelsberger P, Shaw GL, von Stein A (1998) *Proc Natl Acad Sci USA* 95:7092–7096.
40. Tesche CD, Karhu J (2000) *Proc Natl Acad Sci USA* 97:919–924.
41. Thierry AM, Gioanni Y, Degenetais E, Glowinski J (2000) *Hippocampus* 10:411–419.
42. Shenton ME, Dickey CC, Frumin M, McCarley RW (2001) *Schizophr Res* 49:1–52.
43. Harrison PJ (1999) *Brain* 122:593–624.
44. Shergill SS, Brammer MJ, Williams SCR, Murray RM, McGuire PK (2000) *Arch Gen Psychiatry* 57:1033–1038.
45. Ghazanfar AA, Krupa DJ, Nicolelis MA (2001) *Exp Brain Res* 141:88–100.
46. Paxinos G, Watson C (1997) *The Rat Brain in Stereotaxic Coordinates* (Academic, San Diego).
47. Ghazanfar AA, Stambaugh CR, Nicolelis MA (2000) *J Neurosci* 20:3761–3775.
48. Martin JH (1991) *Neurosci Lett* 127:160–164.
49. Kohonen T (1997) *Self-Organizing Maps* (Springer, New York).
50. Demuth H, Beale M (1998) *Neural Network Toolbox User's Guide* (Mathworks, Natick, MA).